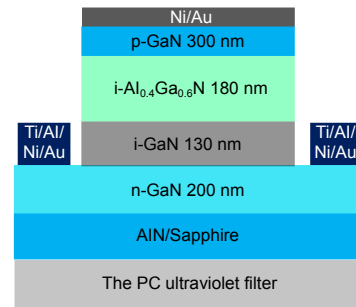




AlGaN solar-blind APD with low breakdown voltage

Kexiu Dong^{1,3}, Dunjun Chen^{1,3*}, Yangyi Zhang¹, Yizhe Sun¹ and Jianping Shi^{2*}

¹School of Electronic and Electrical Engineering, Chuzhou University, Chuzhou 239000, China; ²College of Physics and Electronic Information, Anhui Normal University, Wuhu 241000, China; ³Key Laboratory of Advanced Photonic and Electronic Materials, School of Electronic Science and Engineering, Nanjing University, Nanjing 210093, China



Abstract: A p-i-n type AlGaN heterostructure avalanche photodiodes (APDs) is proposed to decrease the avalanche breakdown voltage and to realize higher gain by using high-Al-content AlGaN layer as multiplication layer and low-Al-content AlGaN layer as absorption layer. The calculated results show that the designed APD can significantly reduce the breakdown voltage by almost 30%, and about sevenfold increase of maximum gain compared to the conventional AlGaN APD. The noise in designed APD is also less than that in conventional APD due to its low dark current at the breakdown voltage point. Moreover, the one-dimensional (1D) dual-periodic photonic crystal (PC) with anti-reflection coating filter is designed to achieve the solar-blind characteristic and cutoff wavelength of 282 nm is obtained.

Keywords: AlGaN; avalanche photodiodes; solar-blind

DOI: 10.3969/j.issn.1003-501X.2017.04.004

Citation: *Opto-Elec Eng.* 2017, **44**(4): 405–409

1 Introduction

AlGaN avalanche photodiodes (APDs) with Al composition more than 40% are being heavily studied because they have intrinsic solar-blindness, which could be a substitute for Si-based photodiodes or photomultiplier tube (PMT) used in ultraviolet (UV) military and scientific fields, such as missile warning and intercepting, flame detection, and ultraviolet optical communication. Over the past twenty years, the performance of AlGaN APDs has made great progress. The p-i-n type AlGaN APD with the gain of 700 was first reported by McClintock et al.^[1] Following, the gain of 1560, 2500 and 4000 for AlGaN APD have been reported successively^[2-4]. In our recent work, we focused on the back-illuminated separate absorption and multiplication (SAM) types AlGaN APDs structure by using the hole-initiated ionization^[5, 6]. To date, the avalanche gain of 2.1×10^4 was achieved successfully^[7].

The development of the solar-blind AlGaN APDs with high gain, however, has been still limited by the low

p-type doping efficiency and high dislocation densities of epitaxial layer. Considering the constraints of material, it is necessary to design the new solar-blind APD structure. Moreover, the breakdown voltages of the AlGaN APDs are generally over 90 V^[8, 9], which can result in a large leakage current. Large dark current not only increases the device noise, but also confines the APDS multiplication gain^[10]. Hence, decreasing the breakdown voltage is very crucial for reducing the leakage, as well as for achieving higher multiplication factors. Recently, we have been devoted to utilizing polarization engineering to enhance the solar-blind separate absorption and multiplication (SAM) AlGaN APD performance by applying the low Al-content AlGaN layer to replace the high Al-content AlGaN as the multiplication layer, and using GaN as the p-type contact layer, as such obtained about 8 V reduction in breakdown voltage under back-illuminated^[6]. In 2016, John Bulmer et al. utilized the polarization engineering to design visible-blind GaN APDs with p-i-i-n structure. It is demonstrated that the avalanche breakdown voltage can be significantly decreased by almost 40%^[11].

In this letter, a back-illuminated p-i-i-n SAM solar-blind AlGaN APD is proposed by using the high Al-content AlGaN as multiplication layer and low Al-content AlGaN as absorption layer. The designed APD

Received 22 November 2016; accepted 5 January 2017

* E-mail: djchen@nju.edu.cn; super-eight@qq.com

can reduce the breakdown voltage and enhance the multiplication gain remarkably. The solar-blind characteristic of this APD can be realized by using one-dimensional photonic crystal (1DPC) structure. The performance of this device including breakdown voltage, gain, energy band, electric field, spectral responsivity and noise are investigated numerically by Silvaco Atlas software.

2 Structure and parameters

Fig. 1(a) shows the schematic of the designed p-i-i-n type solar-blind AlGaN APDs with a 300 nm-thick p-type GaN layer, a 180 nm-thick unintentionally doped $\text{Al}_{0.4}\text{Ga}_{0.6}\text{N}$ multiplication layer, a 130 nm-thick unintentionally doped GaN absorption layer, and 200 nm-thick n-GaN layer. The conventional solar-blind AlGaN APD used here for comparison consists of a p-i-n-i-n structure, as shown in Fig. 1(b). The total thickness of multiplication layer and n-type charge layer of referenced structure is 180 nm, and the thickness of other layers is the same as the designed APD correspondingly. The carrier concentrations for both APDs are $2 \times 10^{18} \text{ cm}^{-3}$ for n-type layers, $1 \times 10^{16} \text{ cm}^{-3}$ for unintentionally doped layers, and $1 \times 10^{18} \text{ cm}^{-3}$ for p-type layer, respectively. In the simulation,

the drift-diffusion model, carrier continuity equation and Poisson equation are used to analyze the charge transport. The carrier generation-recombination models including radiative recombination, SRH recombination and Auger recombination are taken into account. Four types of dark current mechanisms, the choice of polarization charge densities, the ionization and absorption coefficients, and the band-to-band parameters can be found in our previous work^[12].

3 Simulation and analyses

The current-voltage curves of designed APD and conventional AlGaN APD under dark and back-illuminated 275 nm UV-light are calculated and shown in Fig. 2(a). The area for the both APDs is set $225 \mu\text{m}^2$. The power density of incident UV-light is $4 \times 10^{-4} \text{ W/cm}^2$. From Fig. 2(a), it can be seen that the conventional APD needs a high breakdown voltage of 106 V to reach the critical field of ionization. However, the breakdown voltage for designed p-i-i-n APD drops significantly to 76 V. The maximum gain value is 1.12×10^6 for designed APD and 1.65×10^5 for conventional APD, showing an about sevenfold increase. Here, the avalanche multiplication gain is defined as in

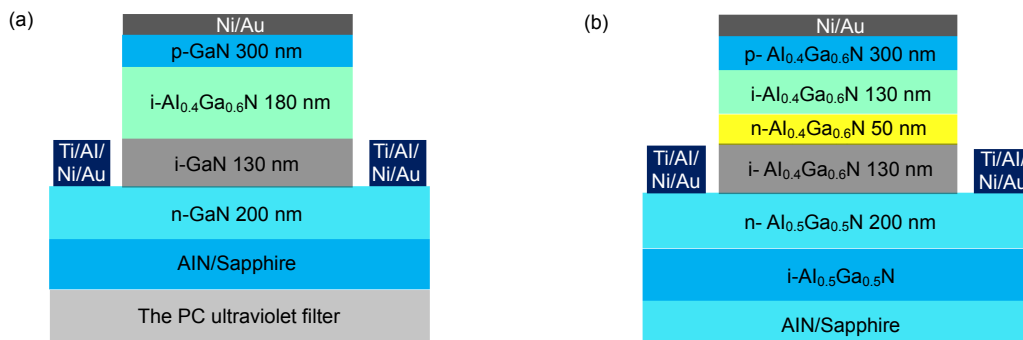


Fig. 1 Schematic of (a) the designed solar-blind APD and (b) conventional AlGaN APD.

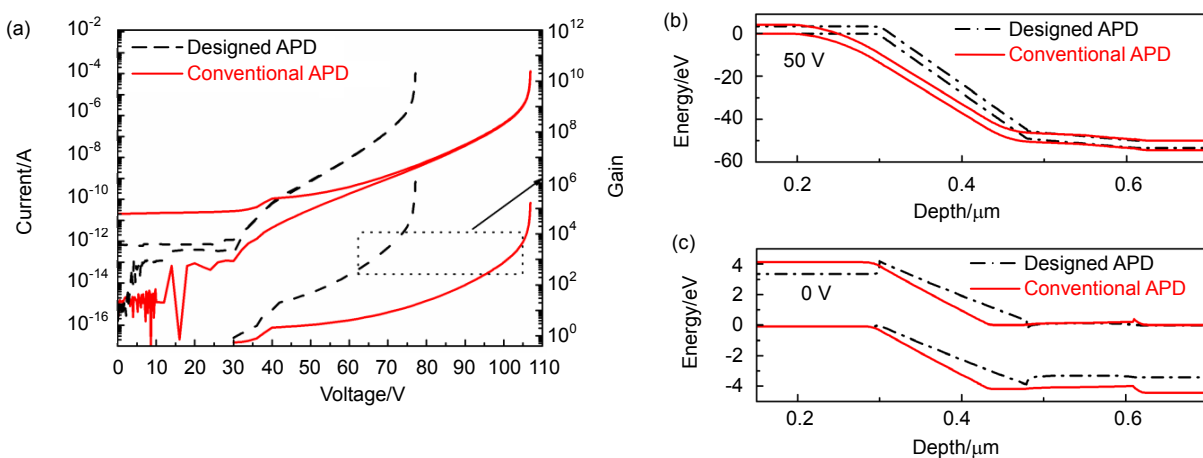


Fig. 2 (a) Reverse I - V curves of designed APD, conventional APD and bias-dependent gain characteristics. The energy band diagrams for both APDs at a reverse bias of (b) 50 V and (c) 0 V.

Ref. [1]. The photocurrent for the designed APD is lower than that of the conventional APD when the reverse-bias is smaller than 40 V. This may be partially due to the thick n-GaN layer in designed APD, which absorbs a large amount of incident light and only a small part of the incident light can cross the n-GaN layer into the absorption layer resulting a low absorption efficiency of light. Another factor may be the large holes barrier that exists between $\text{Al}_{0.4}\text{Ga}_{0.6}\text{N}$ multiplication layer and GaN absorption layer at low operating voltage, which effectively blocks the photo-generated holes in absorption layer into the multiplication layer. As the applied voltage increases, the hole barrier appears. These can be seen from the energy band diagram of both APDs at different bias as displayed in Figs. 2(b) and 2(c). In addition, the depletion layer can extend to the n-GaN layer at large operating voltage. Hence, the effective photo-generated electron-hole pairs are enhanced. The photocurrent increases rapidly. The calculated dark current is 1.04×10^{-4} A for designed APD and 1.22×10^{-4} A for conventional APD at the breakdown voltage.

In order to analyze the effects of polarization engineering on the performance of device, we calculated the electric field distributions of designed APD at different densities of interface charges between p-GaN/i- $\text{Al}_{0.4}\text{Ga}_{0.6}\text{N}$ and i- $\text{Al}_{0.4}\text{Ga}_{0.6}\text{N}$ /i-GaN at the breakdown voltage point. The electric field in multiplication layer increases with the interface charge as shown in Fig. 3(a). This is because the polarization-induced charge at p-GaN/i- $\text{Al}_{0.4}\text{Ga}_{0.6}\text{N}$ interface is negative. In contrast, it is positive at i- $\text{Al}_{0.4}\text{Ga}_{0.6}\text{N}$ /i-GaN interface. Both polarization-induced electric fields in multiplication layer are consistent with those of the build-in electric field and applied reverse-bias field. The total field in multiplication layer, hence, increases, which results in the enhancement of ionization rate together with the gain of APD. Meanwhile, the extra polarization field is beneficial for decreasing the required magnitude of breakdown voltage as demonstrated in table 1. From Fig. 3(a), it can be also deduced that the voltage drop in p-GaN and n-GaN layers reduces with the increased interface charges due to the direction of polarization field opposed to those of the build-in electric field and applied voltage field, which further reduces the breakdown voltage. The reduction of avalanche breakdown voltage is an advantage for decreasing the dark current. Fig. 3(b) presents the strength of electric field for designed APD and conventional APD at breakdown voltage. Although the electric field in multiplication layer for designed APD is slightly lower than that of conventional APD, the hole ionization (α_h) and its product with multiplication layer thickness is larger than that of conventional APD, therefore, shows an enhanced multiplication gain.

Noise analyses are performed for both APDs at the breakdown voltage as shown in Fig. 4. The four general noise mechanism, including diffusion noise, genera-

tion-recombination (GR) noise, impact ionization (II) noise, and Flicker ($1/f$) noise are considered. In this work, the Flicker noise adopts the Hooge model, which is shown as follows^[13]:

$$S_{ID} = \frac{\alpha_H}{N \cdot f} I_D^2, \quad (1)$$

where S_{ID} is the noise spectral densities, N is the number of the free carriers, I_D is the dark current, and α_H is Hooges constant. Hooges constant is proposed to be used as a variable parameter, which in the case of AlGaIn/GaN devices may vary from 10^{-2} ~ 10^{-4} ^[13, 14]. Here, the Hooges constant is set as 10^{-4} . The noise spectral densities of

Table 1 The avalanche breakdown voltage and maximum multiplication gain for the designed APD with different densities of polarization charge at the interface of p-GaN/i- $\text{Al}_{0.4}\text{Ga}_{0.6}\text{N}$ and i- $\text{Al}_{0.4}\text{Ga}_{0.6}\text{N}$ /i-GaN.

Density of polarization charge/cm ²	Voltage/V	Gain
1.1×10^{13}	77	1.12×10^6
9.0×10^{12}	85	3.9×10^5
3.5×10^{12}	110	2.2×10^5
0	125	5.5×10^4

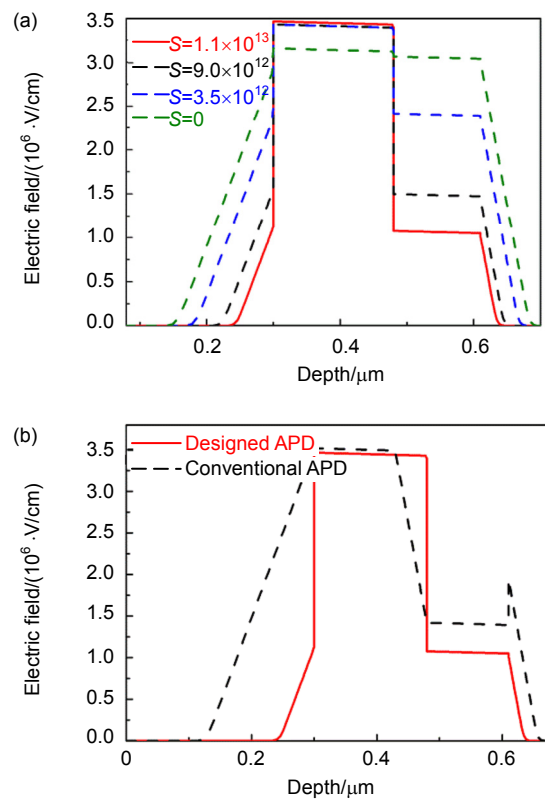


Fig. 3 The electric field distributions of (a) designed APD at different densities of interface charges between p-GaN/i- $\text{Al}_{0.4}\text{Ga}_{0.6}\text{N}$ and i- $\text{Al}_{0.4}\text{Ga}_{0.6}\text{N}$ /i-GaN, and (b) designed APD and conventional APD under breakdown voltage.

impact ionization noise are expressed as $S_{av} = \frac{2qI}{(2\pi f \cdot t)^2}$.

From Fig. 4, we can see that at low frequency the noise characteristics for both APD are dominated by the $1/f$ noise and avalanche noise. For designed APD, the $1/f$ noise and avalanche gain are slightly lower than that of conventional APD, which may be due to the lower elec-

tric field in multiplication layer, as observed in Fig. 3(b). The lower electric field in multiplication layer causes the lower carrier ionization rate, obtaining a lower noise in this device. In addition, the hole $1/f$ (h $1/f$) and diffusion (h diff) noise in both APD are several orders of magnitude higher than that of electron, verifying the hole-initiated multiplication in these structures.

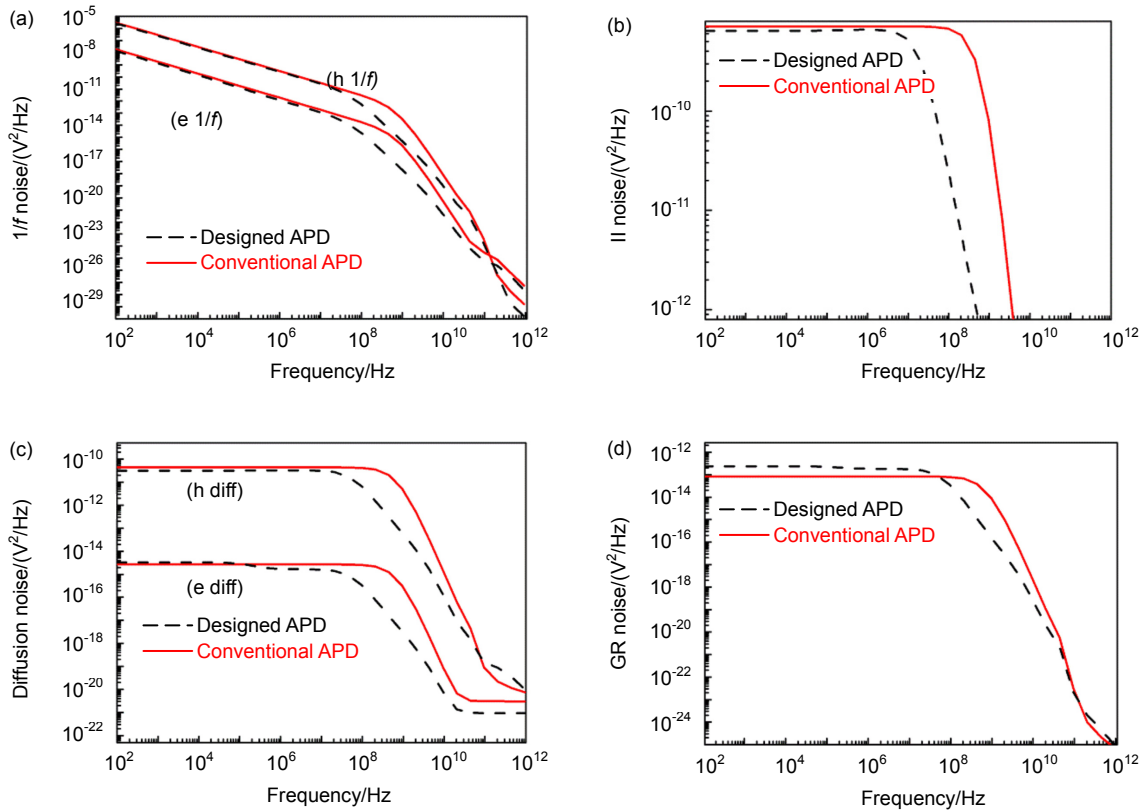


Fig. 4 (a) $1/f$, (b) impact ionization (II), (c) diffusion, and (d) generation-recombination (GR) noise spectral densities at the breakdown voltage.

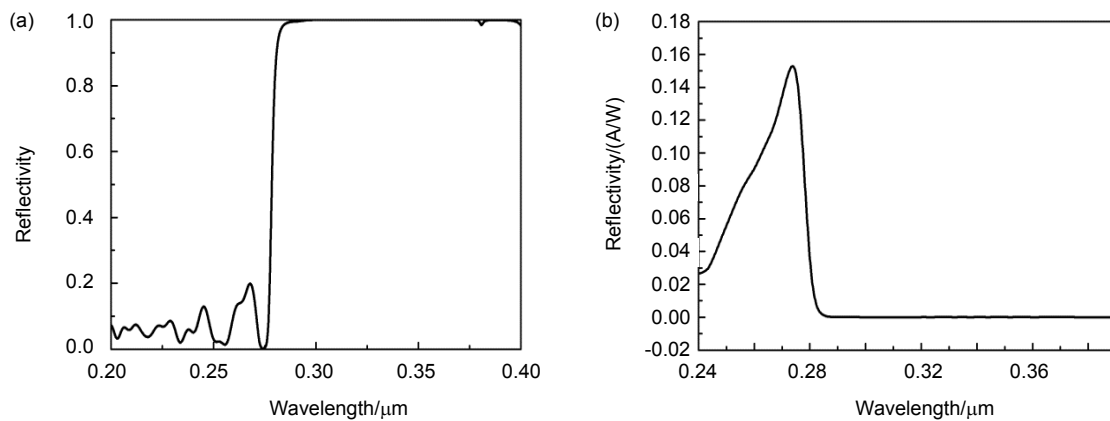


Fig. 5 (a) Reflectivity spectrum of 1D dual-periodic PC filter. (b) Spectral responsivity of the designed APDs.

For the purpose of realizing the solar-blind characteristic of designed APD, we employed the one-dimensional (1D) dual-periodic photonic crystal (PC) with anti-reflection coating structure as a filter stacked by $\text{Si}_3\text{N}_4/\text{SiO}_2$. The refractive index for Si_3N_4 and SiO_2 are 2.01 and 1.46, respectively. The structure of 1D PD filter is $[1.05 \times (L_1/2 \text{ H}_1 \text{ L}_1/2)]_2 (L_1/2 \text{ H}_1 \text{ L}_1/2)_{10} (L_2/2 \text{ H}_2 \text{ L}_2/2)_7 [1.25 \times (L_1/2 \text{ H}_1 \text{ L}_1/2)]$, where L_1 and L_2 represent SiO_2 with the thickness of $\lambda_1/(4 \times 1.46)$ and $\lambda_2/(4 \times 1.46)$, H_1 and H_2 represent Si_3N_4 with the thickness of $\lambda_1/(4 \times 2.01)$ and $\lambda_2/(4 \times 2.01)$. The center wavelengths of λ_1 and λ_2 are 320 nm and 365 nm, respectively. The detailed designing principles can be found elsewhere^[12]. In Fig. 5(a), we calculated the reflectivity spectrum of PC filter by transfer matrix method (TMM). The filter has a high reflectance over 99% with the wavelength of incident light varying from 285 nm to 398 nm, and less than 20% reflectivity when $\lambda < 272$ nm. Fig. 5(b) shows the spectral responsivity of designed APD with PC filter on the back of its sapphire substrate under back illumination at a reverse bias of 0 V. The APD exhibits a peak response of 276 nm and a sharp cut off of 282 nm. So the solar-blind property can be obtained for designed APD, which attributes to the high reflectivity of PC filter with λ in the range of 285 nm to 398 nm.

4 Conclusions

In conclusion, we propose a p-i-i-n AlGaIn SAM APD structure using a high-Al-content AlGaIn layer as multiplication layer and low-Al-content AlGaIn layer as absorption layer by introducing polarization engineering to obtain the lower breakdown voltage and higher avalanche gain. The designed APD exhibits almost 30% reduction of breakdown voltage and about sevenfold increase of gain compared to the conventional AlGaIn APDs. Simultaneously, the designed APD shows the potential advantage to decrease the APD noise. Moreover, the solar-blind characteristic of designed APD is achieved by exploiting 1D dual-periodic PC filter with anti-reflection coating structure.

Acknowledgements

This work was supported by Anhui University Natural Science Research Project, China (KJ2015A153); Initial research fund from Chuzhou University, China (2014qd024); The Higher Education Excellent Youth Talents Foundation of Anhui Province (gxyqZD2016329); the Anhui Provincial Natural Science Foundation of China under Grant (1708085MF149).

References

- 1 McClintock R, Yasan A, Minder K, *et al.* Avalanche multiplication in AlGaIn based solar-blind photodetectors[J]. *Applied Physics Letters*, 2005, **87**(24): 241123.
- 2 Tut T, Gokkavas M, Inal A, *et al.* $\text{Al}_x\text{Ga}_{1-x}\text{N}$ -based avalanche photodiodes with high reproducible avalanche gain[J]. *Applied Physics Letters*, 2007, **90**(16): 163506.
- 3 Sun Lu, Chen Jinlin, Li Jianfei, *et al.* AlGaIn solar-blind avalanche photodiodes with high multiplication gain[J]. *Applied Physics Letters*, 2010, **97**(19): 191103.
- 4 Huang Zeqiang, Li Jianfei, Zhang Wenle, *et al.* AlGaIn solar-blind avalanche photodiodes with enhanced multiplication gain using back-illuminated structure[J]. *Applied Physics Express*, 2013, **6**(5): 054101.
- 5 Huang Y, Chen D J, Lu H, *et al.* Back-illuminated separate absorption and multiplication AlGaIn solar-blind avalanche photodiodes[J]. *Applied Physics Letters*, 2012, **101**(25): 253516.
- 6 Dong Kexiu, Chen Dunjun, Lu Hai, *et al.* Exploitation of polarization in back-illuminated AlGaIn avalanche photodiodes[J]. *IEEE Photonics Technology Letters*, 2013, **25**(15): 1510–1513.
- 7 Shao Zhenguang, Chen Dunjun, Liu Yanli, *et al.* Significant performance improvement in AlGaIn solar-blind avalanche photodiodes by exploiting the built-in polarization electric field[J]. *IEEE Journal of Selected Topics in Quantum Electronics*, 2014, **20**(6): 3803306.
- 8 Shao Zhenguang, Chen Dunjun, Lu Hai, *et al.* High-gain AlGaIn solar-blind avalanche photodiodes[J]. *IEEE Electron Device Letters*, 2014, **35**(3): 372–374.
- 9 Tut T, Yelboga T, Ulker E, *et al.* Solar-blind AlGaIn-based p-i-n photodetectors with high breakdown voltage and detectivity[J]. *Applied Physics Letters*, 2008, **92**(10): 103502.
- 10 Wang Ling, Bao Xichang, Zhang Wenjing, *et al.* Effects of the intrinsic layer width on the band-to-band tunneling current in p-i-n GaN-based avalanche photodiodes[J]. *Semiconductor Science and Technology*, 2009, **24**(9): 095006.
- 11 Bulmer J, Suvama P, Leathersich J, *et al.* Visible-blind APD heterostructure design with superior field confinement and low operating voltage[J]. *IEEE Photonics Technology Letters*, 2016, **28**(1): 39–42.
- 12 Dong Kexiu, Chen Dunjun, Jin Biaobing, *et al.* $\text{Al}_{0.4}\text{Ga}_{0.6}\text{N}/\text{Al}_{0.15}\text{Ga}_{0.85}\text{N}$ separate absorption and multiplication solar-blind avalanche photodiodes with a one-dimensional photonic crystal filter[J]. *IEEE Photonics Journal*, 2016, **8**(4): 6804307.
- 13 Choi H S. Mobility degradation effect to Hooge's constant in recessed-gate $\text{Al}_2\text{O}_3/\text{AlGaIn}/\text{GaIn}$ MIS power transistors[J]. *IEEE Electron Device Letters*, 2014, **35**(6): 624–626.
- 14 Crupi F, Magnone P, Strangio S, *et al.* Low frequency noise and gate bias instability in normally OFF AlGaIn/GaN HEMTs[J]. *IEEE Transactions on Electron Devices*, 2016, **63**(5): 2219–2222.